

Label-free quantitation of phosphopeptide changes in erythrocyte membranes: towards molecular mechanisms underlying deformability alterations in stored red blood cells

While the probability of troublesome adverse effects related to the transfusion of older red blood cell (RBC) units is still a matter of debate and of clinical investigation, what is now known for certain is that blood storage affects the biochemical and biological properties of RBCs. The accumulating changes, collectively known as “storage lesions”, include alterations to either functionality (essentially metabolism and oxygen delivery capacity), or morphology (transition from a discoid to a spherocytic phenotype). These latter are mostly irreversible and result in a more rigid cell structure, with cytoskeleton disorders and perturbation of membrane protein interactions; therefore, they are likely the most responsible for reducing transfusion efficacy. Protein phosphorylation is known to be one of the most important and better-studied posttranslational modifications that affect protein-protein binding interfaces. Interestingly, all components of the red cell membrane skeleton (except actin) are phosphoproteins.¹ Past research has demonstrated that their phosphorylation is involved in the mechanical properties of the erythrocyte membrane.²⁻⁴ However, there have been no studies at all on the phosphorylation events occurring during *in vitro* RBC aging. Based on these considerations, we aimed to investigate the phosphorylation status of erythrocyte membranes while undergoing blood storage for transfusion purposes by means of phosphoproteomics technologies. To this end, we decided to apply a gel-free shotgun proteomics approach to obtain qualitative phosphorylation site mapping of RBC ghosts. Specifically, packed RBCs were lysed with 9 vol of cold 5 mM phosphate buffer pH

8.0 containing 1 mM EDTA, 1mM phenylmethanesulfonyl fluoride (PMSF) and phosphatase inhibitor cocktails (P5726, P0044 Sigma-Aldrich). Two hundred micrograms of red cell membrane proteins were subjected to in-solution tryptic digestion⁵ followed by selective pre-enrichment of phosphorylated peptides through TiO₂ affinity chromatography microcolumns.⁶ Eluted phosphopeptides were then analyzed by LC-MS/MS with both electron transfer dissociation (ETD) and neutral-loss triggered MS³ in collision-induced dissociation (CID), as previously reported.⁷ Experiments were performed in triplicate at 0-day storage time with five leuko-reduced CPD-SAGM RBC units (biological replicates) collected from different donors. Results are shown in Table 1. As expected, pTyr occurrence was very low, but in agreement with the estimated percentage,⁸ while numerous Ser/Thr phosphopeptides were identified. Five of these were chosen to be quantitatively monitored during storage (at 0, 21 and 35 days); selection criteria are described in Table 1. The analytical strategy adopted for the quantitation consisted in a targeted approach because we only quantified (by LC-MS) those individual peptide ions of interest that had been detected and identified previously in data-dependent LC-MS/MS experiments. In detail, targeted quantification was performed by adopting a conventional label-free MS-based workflow relying on the calculation of the extracted ion chromatogram (EIC) peak height from LC-MS runs.^{9,10} To minimize technical variability, each sample (i.e. 200 µg of digested erythrocyte membrane proteins) were spiked with 25 fmol/µg of bovine α-casein digest prior to TiO₂ enrichment. Among the α-casein phosphopeptides detected, the one showing the lower coefficient of variation (CV) was chosen as internal standard for data normalization (i.e. YKVPQLEIVPNSpAEER, m/z 976.40, CV = 14%). Figure 1 shows graphs obtained by plotting the normalized ion intensities of each phosphopeptide *versus* storage time. Measurements of phosphopeptide intensity variation

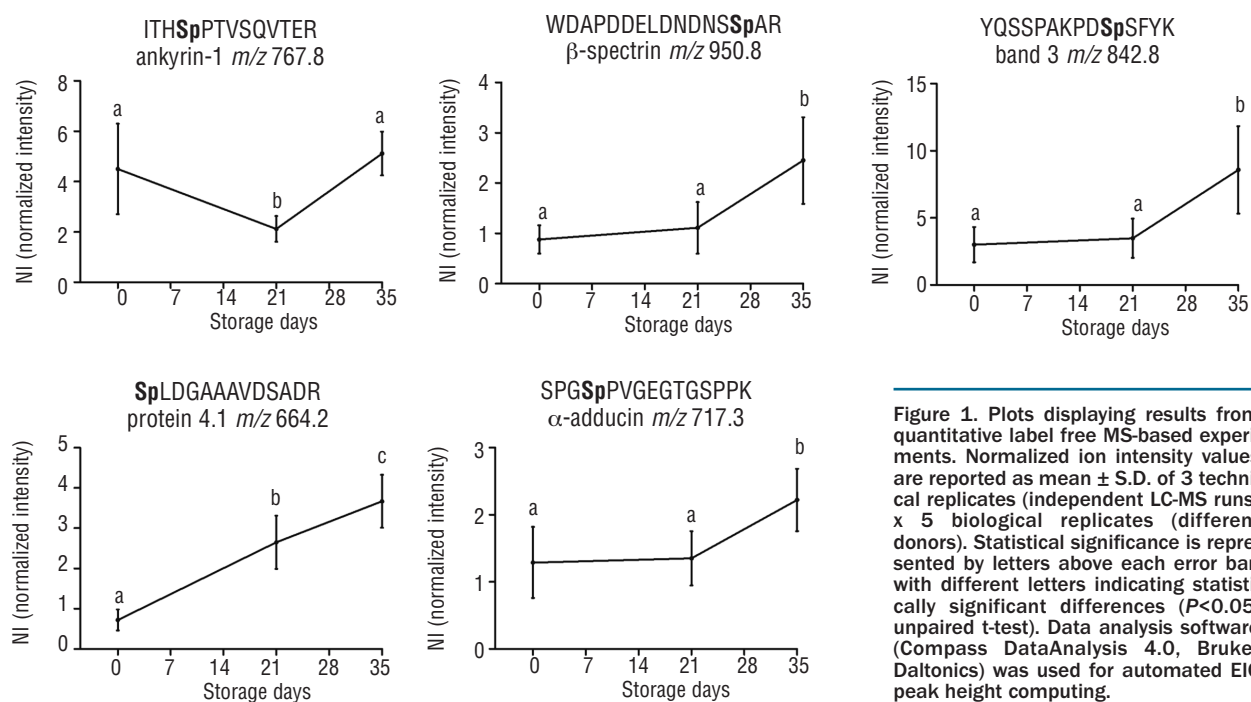


Figure 1. Plots displaying results from quantitative label free MS-based experiments. Normalized ion intensity values are reported as mean \pm S.D. of 3 technical replicates (independent LC-MS runs) \times 5 biological replicates (different donors). Statistical significance is represented by letters above each error bar, with different letters indicating statistically significant differences ($P < 0.05$, unpaired t-test). Data analysis software (Compass DataAnalysis 4.0, Bruker Daltonics) was used for automated EIC peak height computing.

Table 1. Qualitative phosphopeptide mapping by LC-MS/MS in red cell membranes at 0-day storage.^a

Protein ID (NCBI nr Accession N.)	m/z	Charge state	Phosphopeptide sequence	Mascot score	Donor 1	Donor 2	Donor 3	Donor 4	Donor 5
ankyrin-1 (gil70780359)									
	474.75	2+	TpPTPLALR	40 (ETD); 47 (NL)	X		X	X	
	526.73	2+	GASpPNVSNVK	36 (ETD); 67 (NL)			X	X	
	644.37	2+	LGYISpVTDVLK	56 (ETD); 75 (NL)	X	X			
	512.25	3+	ITHSpPTVSQVTER	90 (ETD); 82 (NL)		X	X	X	X
	767.86	2+	ITHSpPTVSQVTER	102 (ETD); 80 (NL)	X	X	X	X	X
	571.60	3+	GEIVNMLEGSGRQSpR	70 (ETD); 50 (NL)	X			X	X
	1004.97	2+	NGASpPNEVSSDGTTPLAIAK	87 (ETD)		X			
	659.77	4+	RQDDATGAGQDSpENEVSLVSGHQQR	133 (ETD); 68 (NL)		X	X		
	582.93	3+	LSTpPPPLAEEGLASR	79 (ETD); 58 (NL)		X	X		
	827.35	3+	QDDATGAGQDSpENEVSLVSGHQQR	45 (NL)				X	X
spectrin beta chain (gil67782319)									
	962.40	2+	LSSSpWESLQPEPSHPY	76 (ETD); 64 (NL)	X		X	X	X
	668.60	3+	LSpSspWESLQPEPSHPY	70 (ETD); 56 (NL)		X	X	X	X
			LSSpSpWESLQPEPSHPY	66 (ETD); 70 (NL)					
	1042.38	2+	LSpSspWESpLQPEPSHPY	37 (ETD)	X	X	X		X
	922.45	5+	QIAERPAEETGPOEEEGETpAGEAPVSHHAATERTSPVSLWSR	61 (ETD)		X			
	950.81	2+	WDAPDELDNDNSpAR	104 (ETD)	X	X	X	X	X
	633.87	3+	WDAPDELDNDNSpAR	98 (ETD); 92 (NL)	X	X		X	X
	556.77	2+	TSpPVLWSR	55 (ETD)			X	X	X
	822.13	4+	DASVAEAWLIAQEPYASGDFGHTVDSpVEK	57 (NL)				X	
	652.29	4+	AWLQDAHRLLSpGEDVQGDEGATR	42 (ETD)					X
band 3 anion transport protein (gil4507021)									
	842.89	2+	YQSSPAKPDSpSFYK	91 (ETD); 44 (NL)	X	X	X	X	X
	562.25	3+	YQSSPAKPDSpFYpK	47 (ETD)			X	X	X
	614.32	3+	RYQSSPAKPDSpSFYK	82 (ETD); 42 (NL)			X		
			RYQSSPAKPDSpFYK	72 (ETD); 40 (NL)		X	X		
	827.59	5+	YQSSPAKPDSpFYKGLDLNGPDDPLQQTGQLFGGLVR	49 (ETD)		X			
alpha-adducin (gil559044)									
	717.30	2+	SPGSpPVGEGTGSPPK	76 (ETD); 110 (NL)	X	X	X	X	X
	728.28	2+	QKGSpeENLDEAR	100 (ETD)	X		X	X	
	613.65	3+	AAVTSpPPPTTAPHKER	90 (ETD); 56 (NL)			X	X	
	777.40	2+	AAVTSpPPPTTAPHK	50 (ETD)		X	X		
	786.80	2+	GDEASEEGQNGSpPK	69 (ETD); 32 (NL)				X	
	600.24	2+	GSpEENLDEAR	53 (ETD)			X		
	762.63	3+	WLNSGRGDEASEEGQNGSpPK	59 (ETD); 39 (NL)	X		X		
	763.87	4+	SPGSpPVGEGTGSPPKWQIGEQEFeALMR	50 (ETD)	X			X	
	908.64	4+	YSDVEVPASVTGYFASDGDGSGTCSpPLRHSFQK	54 (NL)				X	
dematin (gil62089016; gil166706883)									
	523.01	4+	SpLDRTPFHTSLHQGTSK	114 (ETD); 63 (NL)	X	X		X	
	770.25	3+	RGAEEDDDSpGEEMoxK	90 (ETD)	X	X		X	X
	571.28	2+	HLSpAEDFSR	53 (ETD); 55 (NL)		X		X	
	677.32	2+	QRESpVGGSPQTK	55 (ETD)	X	X	X		
	662.84	2+	GNSpLPCVLEQK	41 (NL)	X		X		X
	864.67	4+	LQSTpEFSPSGSETGSPGLQIYPYEMoxLVVTNK	40 (ETD); 70 (NL)					
			LQSpTEFSPSGSETGSPGLQIYPYEMoxLVVTNK	55 (ETD)	X				X
	509.27	2+	SSSpPAYGR	46 (NL)			X	X	
	507.59	3+	TPFHTSpLHQGTSK	91 (ETD)	X	X			
	718.25	3+	GAEEDDDSpGEEMoxK	86 (ETD); 73 (NL)			X		X

continued on the next page

continued from the previous page

protein 4.1 (gil42716291)								
664.28	2+	Sp LDGAAAVDSADR	64 (ETD); 108 (NL)	X	X	X	X	X
410.55	3+	HHASp iSELKK	76 (NL)		X		X	
954.94	4+	SLDGAAAVD Sp ADRSRPRTSAPAITQGGQVAEGVLDASAK	56 (NL)					X
394.22	3+	RLSp THSPFR	51 (ETD)		X	X		
596.64	3+	QASp ALIDRPAPHFER	64 (ETD)	X	X			
glycophorin alpha (gil225711)								
1129.62	3+	KSPSDVKPLPSPD T DVPL Sp VEIENPETS DQ	137 (NL)	X	X	X		
815.60	4+	SPSDVKPLP Sp PDT D VPL Sp VEIENPETS DQ SPSDVKPLP Sp PDT Tp DVPL Sp VEIENPETS DQ	68 (ETD); 84 (NL) 80 (ETD)				X	X X
spectrin alpha chain (gil115298659)								
563.77	2+	KESp LNEAQK	42 (ETD); 60 (NL)	X	X			
413.70	2+	WGS pLQR	37 (ETD)		X	X		
769.86	2+	WGS pLQRLADEQR	63 (NL)					X
hCG2041529 protein (gil119591886)								
862.84	2+	DGV Sp LGA VSp STEEASR	93 (ETD); 70 (NL)		X			X
902.81	2+	DGV Sp LGA VSp STEEASR	50 (NL)		X			X
glycophorin C (gil183327)								
929.74	3+	GTEFAESADAALQGD PALQD AGD SSp PRK	73 (NL)		X	X	X	X
aquaporin (gil688358)								
798.00	3+	V WTSp GQVEEYDL D ADD INSR V WTSp GQVEEYDL D ADD INSp R	48 (ETD) 66 (ETD); 42 (NL)	X	X	X	X	
chain D, Structure And Control Of The Actin Regulatory Wave Complex (gil313103963)								
478.60	3+	GGSGSGGGGGGG Sp GGSK	54 (ETD)	X				X
KIAA0233 protein (gil1510143)								
707.30	2+	SGSp EEAVTDPGER	58 (NL)			X		X
glucose transporter glycoprotein (gil183303)								
860.37	2+	Tp PEELFHPLGAD SQV Tp PEELFHPLGAD Sp Q V	52 (ETD); 51 (NL) 61 (NL)		X	X		X
erythroid membrane-associated protein (gil15808373)								
704.34	2+	Sp EE SIV PRPEGK	57 (ETD)	X	X			
HSP 90 (gil33987931)								
787.52	2+	I EDV Sp DEEDDSGK	51 (ETD); 79 (NL)			X	X	X

^aWhole blood (450 mL ± 10%) was collected from 5 healthy volunteer donors [male = 3, female = 2, age 40 ± 11.2 (mean ± SD)] into CPD (citrate-phosphate-dextrose) anticoagulant (63 mL). After separation of plasma and buffy coat by centrifugation, leukocyte-filtered RBCs were suspended in 100 mL of SAG-M (saline, adenine, glucose, mannitol) additive solution. RBC units were stored for up to 42 days under standard blood bank conditions (4 ± 2°C) and samples were removed aseptically and used for the subsequent analyses. Only phosphopeptides where the phosphorylation site was confidently determined (Mascot delta score greater than 5) are listed. The presence of each phosphopeptide has been verified in all the 5 donors and annotated in the table with an X. Bold annotations highlight the phosphopeptides chosen for quantitation. Selection was firstly based on the obtained results by Western blotting with anti phospho Ser/Thr antibodies where bands corresponding to spectrin, ankyrin, adducin, band 3 and band 4.1 proteins were the most reactive ones (data not shown). Then, for each of these proteins we selected one representative peptide by considering the maximal confidence in the phosphosite localization (in terms of tandem mass spectral quality) and we combined this parameter with the presence of such a peptide in all the biological replicates. The higher Mascot scores obtained for ETD and/or neutral loss (NL)-triggered product ion spectra are shown in brackets (ion score cut off = 30). The detected pSer:pThr:pTyr ratio was 87.5:10.7:1.8.

across all replicates for each condition resulted in CV values ranging from 16% to 40%. Quantitative data have been validated by multiple reaction monitoring (MRM)-based experiments (data not shown). Although each phosphopeptide showed a distinctive trend, it seems that 21-day storage represents a crucial point for the erythrocyte, when either a decrease or a progressive increase in the phosphorylation status occurs. This may correspond to the intensification of mechanisms inducing reduction of deformability observed during blood storage.¹¹ However,

further investigations are needed to explore the functional effects of these phosphorylative changes on the quality of stored RBCs.

All the phosphopeptides quantitatively monitored in this study map in protein regions essential for the functional and structural organization of the red cell membrane architecture, suggesting that they may be involved in the molecular processes that control shape, flexibility and aggregability in stored RBCs. For example, the phosphopeptide ³³³SpLDGAAAVDSADR³⁴⁵ belonging to band 4.1

falls in the 16 kDa protein domain. Curiously, this region seems to affect band 4.1 interactions with spectrin and actin proteins, in turn influencing membrane stability.^{2,12} On the other hand, band 3³⁴⁷YQSSPAKPDSPFYK³⁶⁰ maps in proximity of one of the contact sites (represented by the sequence³⁴⁸LRRRY³⁴⁷) between CDB3 and the protein 4.1,¹³ thus phosphorylation of band 3 Ser-356 may affect the band 3-band 4.1 interactions. Interestingly, the β -spectrin N-terminal region, where our monitored phosphopeptide²⁸WDAPDDELNDNNSpAR³⁸ maps, is known to serve as the counterpart for the 4.1R binding.¹⁴ As far as α -adducin is concerned, it is known that the its 'neck domain' contains crucial amino acids (Ser-408, Ser-436, Ser-481) whose phosphorylation has previously been seen to favor the detachment of adducin from the spectrin/actin network,³ but the same region is also clearly involved in association of adducin monomers to heterodimers, which constitute the functionally active form of the protein.¹⁵ The α -adducin phosphopeptide monitored in our study (³⁵⁵SPGSpVVGEGTGSPPK³⁶⁹) maps within the neck domain, very close to the sites cited before, thus Ser-358 may either represent a new phosphorylation site with regulatory properties in the adducin oligomerization process, or may be involved in the control of vertical interactions anchoring the junctional complex to the lipid bilayer. On the other hand, still little information is available for the region of ankyrin where the¹⁶⁶³ITHSpPTVSQVTER¹⁶⁹⁵ phosphopeptide is located (downstream a 'death domain' at the C-terminus), thus any hypothesis about its involvement in maintaining membrane stability would, for the moment, be purely speculative given our present knowledge.

In conclusion, our MS-based approach allowed, for the first time, to follow peptide-specific quantitative changes in the phosphorylation status of ghost proteins in preserved RBCs, clearly demonstrating an increase in the Ser/Thr phosphorylation levels of RBC membrane skeletal proteins during blood storage. In our opinion, the investigation of the phosphorylation-triggered molecular events occurring during *in vitro* erythrocyte aging will be of great benefit in elucidating the causes of the reduced survival of transfused RBCs. In this direction, future large-scale phosphoproteomics analyses can provide new biological insights.

Valentina Longo, Cristina Marrocco, Lello Zolla, and Sara Rinalducci

Department of Ecological and Biological Sciences, University of Tuscia, Viterbo, Italy

Correspondence: sara.r@unitus.it/zolla@unitus.it
doi:10.3324/haematol.2013.103333

Key words: erythrocyte, deformability, label-free quantitation, phosphopeptide changes, stored red blood cells.

Funding: the authors would like to thank the Italian National Blood Centre (CNS, Rome) for the financial support.

The online version of this article has a Supplementary Appendix.

Information on authorship, contributions, and financial & other disclosures was provided by the authors and is available with the online version of this article at www.haematologica.org.

References

- Manno S, Takakuwa Y, Nagao K, Mohandas N. Modulation of erythrocyte membrane mechanical function by beta-spectrin phosphorylation and dephosphorylation. *J Biol Chem*. 1995;270(10):5659-65.
- Manno S, Takakuwa Y, Mohandas N. Modulation of erythrocyte membrane mechanical function by protein 4.1 phosphorylation. *J Biol Chem*. 2005;280(9):7581-7.
- Matsuoka Y, Hughes CA, Bennett V. Adducin regulation. Definition of the calmodulin-binding domain and sites of phosphorylation by protein kinases A and C. *J Biol Chem*. 1996;271(41):25157-66.
- Ferru E, Giger K, Pantaleo A, Campanella E, Grey J, Ritchie K, et al. Regulation of membrane-cytoskeletal interactions by tyrosine phosphorylation of erythrocyte band 3. *Blood*. 2011;117(22):5998-6006.
- Zhang H, Lin Q, Ponnusamy S, Kothandaraman N, Lim TK, Zhao C, et al. Differential recovery of membrane proteins after extraction by aqueous methanol and trifluoroethanol. *Proteomics*. 2007;7(10):1654-63.
- Thingholm TE, Jorgensen TJ, Jensen ON, Larsen MR. Highly selective enrichment of phosphorylated peptides using titanium dioxide. *Nat Protoc*. 2006;1(4):1929-35.
- D'Alessandro A, Rinalducci S, Marrocco C, Zolla V, Napolitano F, Zolla L. Love me tender: an Omic window on the bovine meat tenderness network. *J Proteomics*. 2012;75(14):4360-80.
- Olsen JV, Blagoev B, Gnäd F, Macek B, Kumar C, Mortensen P, et al. Global, in vivo, and site-specific phosphorylation dynamics in signaling networks. *Cell*. 2006;127(3):635-48.
- Soderbloom EJ, Philipp M, Thompson JW, Caron MG, Moseley MA. Quantitative label-free phosphoproteomics strategy for multifaceted experimental designs. *Anal Chem*. 2011;83(10):3758-64.
- Quintana LF, Campistol JM, Alcolea MP, Banon-Maneus E, Sol-Gonzalez, Cutillas PR. Application of label-free quantitative peptidomics for the identification of urinary biomarkers of kidney chronic allograft dysfunction. *Mol Cell Proteomics*. 2009;8(7):1658-73.
- Frank SM, Abazyan B, Ono M, Hogue CW, Cohen DB, Berkowitz DE, et al. Decreased erythrocyte deformability after transfusion and the effects of erythrocyte storage duration. *Anesth Analg*. 2013;116(5):975-81.
- Liu J, Guo X, Mohandas N, Chasis A, An X. Membrane remodeling during reticulocyte maturation. *Blood*. 2010;115(10):2021-7.
- Jons T, Drenckhahn D. Identification of the binding interface involved in linkage of cytoskeletal protein 4.1 to the erythrocyte anion exchanger. *EMBO J*. 1992;11(8):2863-7.
- An X, Debnath G, Liu S, Lux SE, Baines A, Gratzler W, Mohandas N. Identification and functional characterization of protein 4.1R and actin-binding sites in erythrocyte beta spectrin: regulation of the interactions by phosphatidylinositol-4,5-bisphosphate. *Biochemistry*. 2005;44(31):10681-8.
- Li X, Matsuoka Y, Bennett V. Adducin preferentially recruits spectrin to the fast growing ends of actin filaments in a complex requiring the MARCKS-related domain and a newly defined oligomerization domain. *J Biol Chem*. 1998;273(30):19329-38.